glacies

MDPI

*Article*

# Two-Step Glaciation of Antarctica: Its Tectonic Origin in Seaway Opening and West Antarctica Uplift

**Hsien-Wang Ou**

Lamont-Doherty Earth Observatory, Columbia University, Palisades, NY 10964, USA; hwo1@columbia.edu

**Abstract:** The Cenozoic glaciation of Antarctica proceeded through two distinct steps around 35 and 15 million years ago. The first icing was attributed to thermal isolation due to the opening of the Drake/Tasman passages and the development of the Antarctic circumpolar current. I also subscribe to this "thermal isolation" but posit that, although the snowline was lowered below the Antarctic plateau for it to be iced over, the glacial line remains above sea level to confine the ice sheet to the plateau, a "partial" glaciation that would be sustained over time. The origin of the second icing remains unknown, but based on the sedimentary evidence, I posit that it was triggered when the isostatic rebound of West Antarctica caused by heightened erosion rose above the glacial line to be iced over by the expanding plateau ice, and the ensuing cooling lowered the glacial line to sea level to cause the "full" glaciation of Antarctica. To test these hypotheses, I formulate a minimal box model, which is nonetheless subjected to thermodynamic closure that allows a prognosis of the Miocene climate. Applying representative parameter values, the model reproduces the observed two-step icing followed by the stabilized temperature level, in support of the model physics.

**Keywords:** Antarctic glaciation; snowline; glacial line; thermal isolation; West Antarctica uplift; Miocene cooling



**Citation:** Ou, H.-W. Two-Step Glaciation of Antarctica: Its Tectonic Origin in Seaway Opening and West Antarctica Uplift. *Glacies* **2024**, *1*, 80–91. https://doi.org/10.3390/glacies1020006

Academic Editor: Steven R. Fassnacht

Received: 9 August 2024
Revised: 24 September 2024
Accepted: 10 October 2024
Published: 12 October 2024



## 1. Introduction

The glaciation of Antarctica in the Cenozoic proceeded through two distinct steps: one around the Eocene–Oligocene boundary (EOB) about 35 million years ago (Ma) when the ice sheet had covered the Antarctic plateau and the second one during the middle Miocene about 15 Ma when the ice sheet expanded to cover the whole Antarctica [1]. The first icing is widely attributed to the opening of the Drake/Tasman passages with the development of the Antarctic circumpolar current (ACC), which curbed the ocean heat from the subtropics to promote ice growth [2–4]. I also subscribe to this "thermal isolation" in the cooling of Antarctica but find it expedient and indeed necessary to distinguish two key physical lines: the snowline (SL) that delimits the lower boundary of net accumulation (no need to distinguish it from the slightly lower equilibrium line for our purpose) and the glacial line (GL) that marks the ice front where the net accumulation is depleted by ablation. Based on mass and energy balances, a previous study [5] has derived an expression for the marking temperature of the GL, coined the "glacial marking temperature" (GMT), which turns out to primarily be an intrinsic property of the ice sheet, and its deduced value of 5 °C is consistent with the current observation [6].

In the parlance of these lines, I posit that the first icing was triggered when the thermal isolation lowered the snowline to below the Antarctic plateau to cause it to ice over but the augmented albedo and attendant cooling had not depressed the glacial line to sea level, so the ice sheet remained confined to the plateau and its flanking slope. This "partial" glaciation represents an equilibrium that would persist over time, as reflected in the stabilized temperature level following its sharp drop during the first icing [7]. Both the posited onset and stabilization of the partial glaciation need to be assessed quantitatively for their plausibility, as attempted in this study.

Unlike the first icing, the origin of the second icing remains unknown since it has long passed the full development of the ACC more than 10 million years prior [8], as attested by the stabilized temperature noted above. Such stability also argues against its attribution to $pCO_2$ [9–11], which generally trends as temperature and has lowered to the present level since ~20 Ma [12]; hence, it may not account for the observed abrupt cooling of about 5 °C through the second icing [7] based on calculated sensitivity [13]. As the second icing is what produces the full glaciation, the missing explanation exposes a significant gap in our understanding of the Antarctic ice sheet, which adversely impacts our ability to assess its stability under anthropogenic warming [14]. It is an attempt to fill this gap that motivates the present study.

In seeking the tectonic origin of the second icing, I take note of the sedimentary evidence that West Antarctica was uplifted by about 1 km in the early Miocene as an isostatic rebound to the heightened erosion ([15–17] and [18] (their Figure 5c)). I also note that West Antarctica has abutted the Antarctic plateau since the early Cenozoic, as seen in the uplift of the Transantarctic mountains (TAM) [19,20]. With these enabling conditions, I posit that the second icing was triggered when West Antarctica rose above GL to be iced over by the expanding ice sheet from the neighboring Antarctic plateau [15], a state termed "partial-plus" glaciation. Furthermore, I posit that the ensuing cooling has lowered the already-low GL to sea level, so the ice sheet descended the slope to grow over lowlands until it covered the entire Antarctica, a state termed "full" glaciation. Just like the partial glaciation after the first icing, this full glaciation is an equilibrium hence was accompanied by a stabilized temperature level until the renewed cooling in the Pliocene, the latter a topic that lies outside the present scope [5]. Again, the posited scenario of the second icing needs to be assessed quantitatively for its plausibility.

To test the above hypotheses in the most transparent manner, I formulate a minimal warm/cold/Antarctic box model in Section 2, which allows the derivation of the Antarctic temperature and glacial regimes. In Section 3, I apply "standard" parameter values to prognose the time evolution of the Miocene climate and to assess the plausibility of two-step icing. I provide additional discussions in Section 4 and conclude the paper in Section 5.

## 2. Methodology

The methodology of this study entails the formulation of a box model and the derivation of the Antarctic temperature and its associated glacial regimes, as provided in the succeeding subsections below.

### *2.1. Box Model*

To isolate the key physics in producing the observed two-step icing of Antarctica, I formulate a minimal box model as sketched in Figure 1 in which the coupled ocean/atmosphere is divided into warm/cold boxes aligned at the subtropical front (set at 30° S) and the cold ocean box is subdivided into cold/Antarctic boxes by the ACC (set at 65° S). In our convention, global means are overbarred, and deviations from the global means (termed "differential") are primed and subscripted 1/2/3 for warm/cold/Antarctic boxes, respectively. The latitudinal distance is defined as $y = \sin(\text{latitude})$, so it is proportional to the area on a sphere.

Retaining only dominant energy balances, the system is heated differentially by the incoming shortwave (SW) flux ($q_i^*$, all symbols are listed in Appendix A), which, after absorption by the atmosphere and reflection by the planetary albedo, is absorbed by the ocean ($q_i$, referred to as "radiative forcing"). This radiative forcing would differentiate the sea surface temperature (SST) to induce poleward ocean heat transport, which is set to zero at the ACC to implement the thermal isolation. The differential SST in turn would differentiate the surface air temperature (SAT) by the convective flux ($q_c$), neglecting, by comparison, the latitudinal variation of the surface and outgoing longwave (LW) fluxes ([21] (their Figure 6.14) and [22] (his Figure 20)). Since the neglected terms do not alter the thermodynamic closure, they do not materially impact the model results.

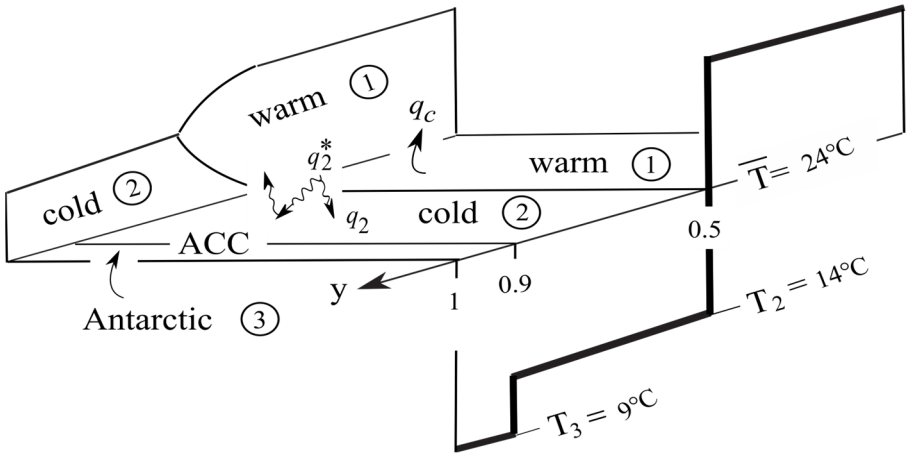


**Figure 1.** The model configuration showing warm/cold/Antarctic ocean boxes of coupled ocean/atmosphere system. The incoming SW flux ($q_i^*$), after the atmospheric absorption and reflection by the planetary albedo is absorbed by the ocean ($q_i$) to differentiate the SST (thick solid line), which in turn differentiates the SAT by the convective flux ($q_c$). The latitudinal coordinate is defined as $y = \sin(\text{latitude})$ hence proportional to the surface area on a sphere, and the SST shown is the EOB solution assuming small and thermal-isolated Antarctic box.

Because of the thermal inertia of the ocean, I neglect its seasonality. Air, however, is strongly warmed in summer by atmospheric absorption, whose temperature remains bounded by the underlying SST in maintaining a radiative-convective equilibrium of the troposphere. This "convective bound" is a distinct feature in observation ([21] (their Figure 10.7, lower panel)), so the SST may serve as a proxy of the co-zonal summer SAT that controls the glacial margin. Given the smallness of the Antarctic box, the SST of the warm/cold boxes is approximately the two-box solution of [23] (see also [5]). For self-containment, some of his derivations are repeated below.

Despite its simplicity, my box model is physically closed to allow a prognosis of the temperature, thus differing from coarse-grained general circulation models (GCMs, see further discussion in Section 4). Specifically, because of inherently turbulent planetary fluids, the climate state is a macroscopic manifestation of a nonequilibrium thermodynamic system hence subjected to maximum entropy production (MEP)—a generalized second law. Readers are referred to [24,25] for reviews of MEP and [5] for its additional justifications and applications in paleoclimate studies. With this support, I am justified to pose MEP as a working hypothesis in our model closure.

### *2.2. Antarctic Temperature*

Since MEP is a selection rule, it can be applied hierarchically, first to the atmosphere and then to the ocean, as discussed sequentially below. For the atmosphere, given the stated energy balance, its irreversible entropy production equals the entropy flux through its lower boundary, which is of the form of $\alpha(T - T_a)/T_a$ where $\alpha$ is the air–sea exchange coefficient set to 10 $\mathrm{Wm}^{-2}\mathrm{K}^{-1}$ [23]. Since the temperature variation is small compared with the global mean (in Kelvins), the inverse temperature in the above expression can be linearized, so the differential entropy production (removing the global mean) varies as (the symbol "~")

$$\sigma_a' \sim \alpha\left(T_2' - T_{a,2}'\right)T_{a,2}', \tag{1}$$

which is expressed in the cold-box variables since the warm-box has the same value. Maximizing this entropy production against $T_{a,2}'$ yields

$$T_{a,2}' = T_2'/2, \tag{2}$$

a well-known result of MEP [24] because of the mutual compensation of the thermodynamic flux (heat transport, the bracketed term) and thermodynamic force (differential temperature).

Having linked SAT to SST, I shall next apply MEP to the ocean to link SST to the differential forcing. The differential heating of the cold ocean box is the radiative forcing minus the convective flux, so the ocean counterpart to (1) is

$$\sigma_o' \sim \left[q_2' - \alpha\left(T_2' - T_{a,2}'\right)\right] T_2'. \tag{3}$$

Applying (2) and maximizing (3) against $T_2'$, we obtain

$$T_2' = q_2'/\alpha, \tag{4}$$

or the cold-box SST varies linearly with the differential forcing. Now, for the Antarctic box that receives no heat from the subpolar ocean, the radiative forcing must be balanced by convective flux, or

$$q_2' - \alpha\left(T_3' - T_{a,2}'\right) = 0, \tag{5}$$

and substituting from (2) and (4) then yields

$$T_3' = s' q_2', \tag{6}$$

where

$$s' \equiv \frac{3}{2\alpha} \tag{7}$$

is the "local" sensitivity linking the Antarctic temperature to the differential forcing with a standard value of 0.15 °C$\left(\mathrm{Wm}^{-2}\right)^{-1}$. Comparing (6) with (4), we see that the thermal isolation renders an Antarctic temperature 50% colder than the cold-box temperature (with respect to the global mean). For the current global mean of 15 °C and a differential forcing of 100 $\mathrm{Wm}^{-2}$ [21], the model solution yields subpolar and Antarctic SST of 5 °C and 0 °C, respectively, in broad agreement with the observed ones [26]. In addition, as seen in [27], the model-deduced meridional overturning circulation depends only on $\alpha$ to yield a transport of 11 Sv for a 6000 km-wide North Atlantic, which is of the same order as the observed one [28]. These observational comparisons constitute veritable tests of MEP as they involve no free parameters. The temperature shown in Figure 1 is the model solution at EOB when the global temperature is set to 24 °C [29], which shows that thermal isolation may cool the Antarctic temperature from 14 °C to 9 °C, a drop of 5 °C consistent with the observed cooling prior to the first icing [7], underscoring its considerable potency.

I shall next examine how the ice albedo would alter the radiative forcing, hence the SST. The radiative forcing of the cold/Antarctic box is

$$q_2 = q_2^*(1 - b - a_2), \tag{8}$$

where $q_2^*$ is the incoming SW flux, $b$ is the atmospheric absorption, and $a_2$ is the planetary albedo; only the latter varies with the ice cover $i$ (in the fraction of the cold-box area) via

$$\delta q_2 = -q_2^* \delta a_2 = -q_2^* \Delta r \delta i, \tag{9}$$

where $\Delta r$ is the excess reflectance of ice over land set to 0.7—neglecting the uncertain cloud effect [30]. Since the cold box spans one-quarter of the global surface, the global forcing varies as

$$\delta \overline{q} = \delta q_2/4, \tag{10}$$

so the differential forcing varies as

$$\delta q_2' \equiv \delta\left(q_2 - \overline{q}\right) = 3\delta q_2/4. \tag{11}$$

Applying (6) and (11), we derive

$$\delta T_3' = s'\delta q_2' = 3s'\delta q_2/4. \tag{12}$$

On the other hand, the global cooling is given by

$$\delta\overline{T} = \overline{s}\delta\overline{q} = \overline{s}\delta q_2/4, \tag{13}$$

where the "global" sensitivity $\overline{s}$ has a range of [0.5, 1.5] $^\circ\mathrm{C}\left(\mathrm{Wm}^{-2}\right)^{-1}$ based on climate models [13], and its median value $\overline{s} = 1\ ^\circ\mathrm{C}\left(\mathrm{Wm}^{-2}\right)^{-1}$ [29] is adopted as our standard value. Combining (12) and (13), and applying (9), we derive the Antarctic cooling

$$\delta T_3 \equiv \delta\left(\overline{T} + T_3'\right) = -s^* q_2^* \Delta r \delta i, \tag{14}$$

where

$$s^* \equiv \left(\overline{s} + 3s'\right)/4 \tag{15}$$

is the "effective" sensitivity of the Antarctic temperature to the changing ice cover. It is seen that the global sensitivity dominates the local sensitivity in contributing to the effective sensitivity, so even for a minimal box model, one may not neglect the global cooling in assessing the Antarctic climate change.

Equation (14) entails the positive albedo-temperature feedback of a continuous system: increasing ice cover would cool the temperature, which in turn propels the ice growth to further cool the temperature. But for a discontinuous system, the feedback is arrested when ice cover attains the over-ridden area to uniquely specify the temperature change; the temperature, on the other hand, selects discrete ice cover, as considered next.

### *2.3. Glacial Regimes*

As noted in Section 1, GMT is an intrinsic ice-sheet property, which specifies the vertical drop of GL from SL, both thus varying in tandem with temperature. Depending on their altitude relative to the plateau and sea level, I discern three glacial states of Antarctica as sketched in Figure 2.

Figure 2a shows the case in which the snowline is lowered below the Antarctic plateau (light shade) to trigger the first icing (polka-dotted). Through albedo-temperature feedback, the ice would grow to cover the plateau, and the ensuing cooling would lower both SL (thick solid) and GL (thick dashed). The GL, however, remains above sea level to confine the ice sheet to the plateau, a state of "partial" glaciation.

Figure 2b shows the case in which West Antarctica (dark shade) rises above the GL to be iced over by the expanding ice sheet from the Antarctic plateau, triggering the second icing. The lowered GL, however, remains above sea level by the ensuing cooling, so the ice sheet is limited to the Antarctic plateau and West Antarctica, a state of "partial-plus" glaciation.

Figure 2c shows the case in which cooling during the second icing has lowered the GL to sea level, so the ice sheet would now descend the slope and grow on the lowland to cover the entire Antarctica, a state of "full" glaciation.

Given the external conditions, these glacial states may or may not be sustained depending on the effective sensitivity (15). To illustrate this, I show in Figure 3 the time evolution of the ice cover when subjected to the two icings (circled numbers). After the first icing, the ice rapidly grows to cover the Antarctic plateau (of area $i_{AP}$), a partial glaciation ($P$) that would be sustained over time if the effective sensitivity is sub-critical (that is, GL remains above sea level); otherwise, the ice sheet would continue to grow (thin solid line) to cover the entire Antarctica (of area $i_A$), which would preclude a second icing.

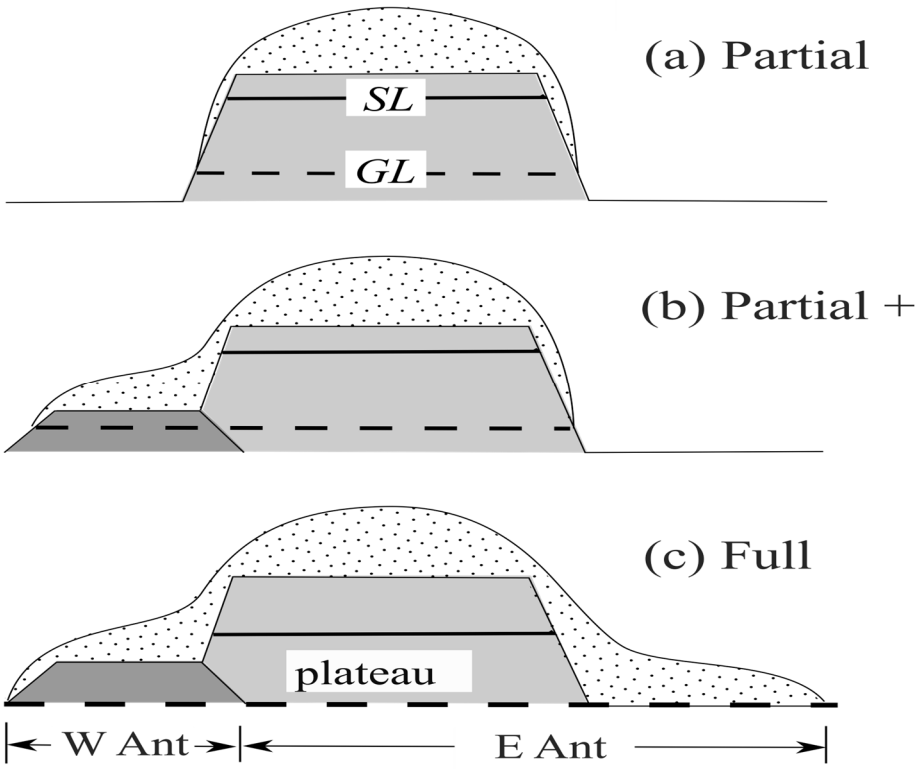


**Figure 2.** Glacial states for Antarctica: (**a**) "partial" glaciation when the ice sheet is confined to the Antarctic plateau; (**b**) "partial-plus" glaciation when the ice sheet covers the Antarctic plateau and West Antarctica; and (**c**) "full" glaciation when the ice sheet covers entire Antarctica.

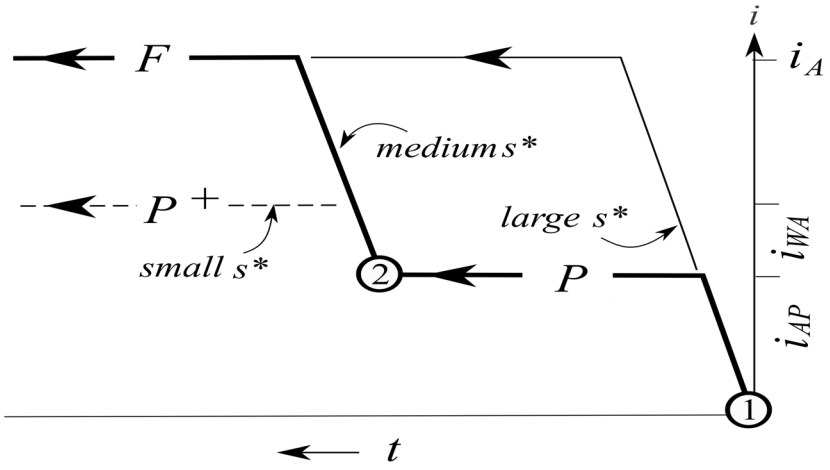


**Figure 3.** Time evolution of the ice cover subjected to the two icings (circled numbers). $P/P^+/F$ are partial/partial-plus/full glaciation, $i_{AP}/i_{WA}/i_A$ are areas of Antarctic plateau/West Antarctica/Antarctica, thin solid/dashed lines are for supercritical/subcritical sensitivity, and thick solid line represents the modeled two-step icing, respectively.

Following the sustained partial glaciation, the second icing is triggered when West Antarctica (of area $i_{WA}$) rises above the GL to be iced over by the expanding plateau ice. This partial-plus ($P^+$) glaciation would be sustained over time (thin dashed line) if the effective sensitivity is sub-critical; otherwise, the GL would descend to sea level to cause full glaciation ($F$, thick solid line). With the thick solid line representing the modeled two-step icing, I shall next assess its plausibility via a quantitative calculation.

## 3. Results

### *3.1. Miocene Climate*

Applying the standard parameter values listed in Appendix A, I calculate and plot in Figure 4 the time evolution of the SST (thick solid line, doubling as summer SAT, hence SL), the GL (thick dashed line), and the ice cover $i$ (dotted, in the fraction of the cold-box area). I have set the first icing at EOB of 35 Ma and the second icing in the mid-Miocene of 15 Ma (thin vertical lines with circled numbers) and the Antarctic plateau (light shade) at 1.5 km [12], so the EOB temperature shown in Figure 1 would trigger the first icing. Since glacial transitions (striped) occur over short mass–balance timescales, they are strongly magnified to aid the visualization. It is seen that the modeled time series have captured broad features of the observed one [1,7]; I, therefore, offer the following interpretation of the Miocene climate based on model physics.

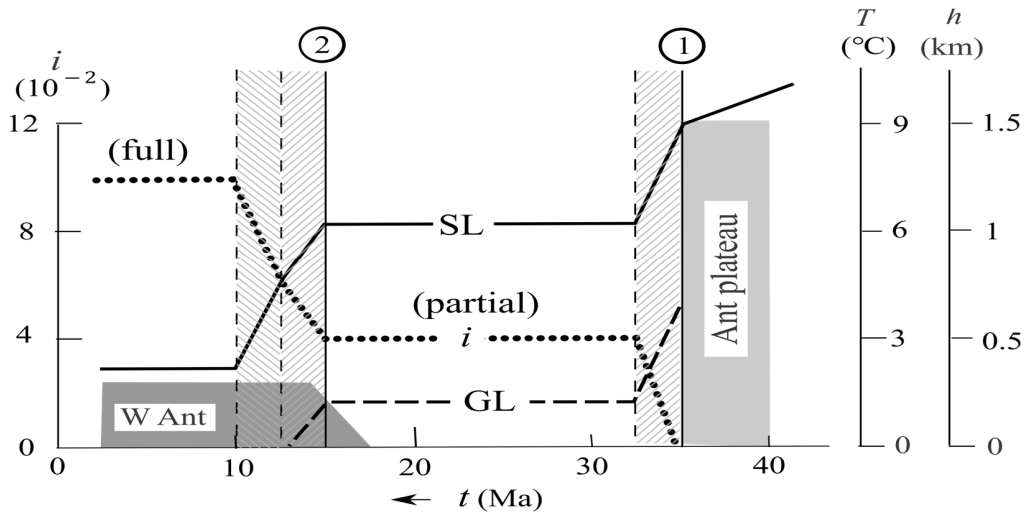


**Figure 4.** Modeled time series of SST (thick solid, doubling as summer SAT hence SL), GL (thick dashed), and ice cover $i$ (dotted, in fraction of the cold-box area), with sustained partial/partial+/full glaciations indicated. Thin vertical lines mark the onset of the two icings (circled numbers): the first when SL falls below the Antarctic plateau (light shade) and the second when West Antarctica (dark shade) rises above GL. Transitions between glacial states (striped) are strongly magnified for visualization.

The first icing is triggered when the thermal isolation due to the gradual opening of the Drake/Tasman passages has lowered the SL to below the Antarctic plateau around EOB, causing it to be iced over. The positive albedo-temperature feedback would cool the SST on the short mass-balance timescale to appear abrupt in the $\delta^{18}$O time series [7]. Since the lowered GL remains above sea level, the ice sheet is confined to the Antarctic plateau, whose vastness causes about 50 m drop in the sea level [1,31]. But the ice sheet, being terrestrial based, only produces episodic ice-rafted debris (IRD) through outlet glaciers [32]. Since this partial glaciation represents an equilibrium state, it is sustained over time until the mid-Miocene with the occurrence of the second icing.

The second icing is triggered when West Antarctica (dark shaded) is uplifted above GL as an isostatic rebound to the heightened erosion in the early Miocene [18]. Since GL has already been lowered to the low hundred meters after the first icing, it may easily be topped by the inferred uplift of 1 km even though the latter may be countered by uncertain thermal subsidence [33]. As West Antarctica has abutted the Antarctic plateau since Oligocene [19], the existing plateau ice sheet provides a ready nucleation for its expansion onto West Antarctica [15]. While blockage by TAM may reduce the ice flux [34], it does not alter the equilibrium ice volume, a function mainly of its covered area, and then the slowed icing, being governed by mass balance, remains abrupt hence does not discernibly impact the time evolution. Although West Antarctica is quite smaller than the Antarctic plateau to cause only minor cooling, the latter is nonetheless sufficient to propel the already-low GL

to sea level, so the ice sheet, after covering West Antarctica, would descend the slope and grow on Antarctic lowlands to cover the entire Antarctica. Given the sizable ice expansion, it generates strong signals in both $\delta^{18}$O and sea level records that are commensurate with the first icing [1,31], but, in contrast, the ice sheet is now marine-based to cause massive deposition of IRD [32,35].

The full glaciation represents an equilibrium hence it persists to the present [36], but the stabilized SST remains about 2 °C above the freezing point, as observed [29]. A renewed cooling in the Pliocene would cool it to the present freezing point [7], a precondition for the observed formation of vast ice shelves. The Pliocene cooling has been attributed to the uplift of the Tibetan highlands [5], a topic that however lies beyond the scope of the present study. The glaciation of West Antarctica would depress much of it to below sea level, as is the current case, which need not conflict with its putative uplift in the early Miocene and, in any case, West Antarctica must be above sea level to host the initial glaciation [33,34].

### *3.2. Model Sensitivity*

Although standard parameter values have replicated the observed two-step icing, it is seen from Figure 3 that it depends on whether GL is above/below sea level or, equivalently, whether the Antarctic temperature is above/below the GMT, referred to as sub/super-critical. With the box model filtering out peripheral parameters, it is readily seen that the main uncertainty lies in the effective sensitivity, and the observed two-step icing requires it to be subcritical after the first icing but supercritical after the second icing. From (14), these two conditions thus state

$$T_{3,in} - s^* q_2^* \Delta r i_{AP} \geq T_g, \tag{16}$$

and

$$T_{3,in} - s^* q_2^* \Delta r (i_{AP} + i_{WA}) \leq T_g, \tag{17}$$

where $T_{3,in}$ is the "initial" Antarctic temperature at EOB (=9 °C) when the first icing is triggered. As such, the effective sensitivity must lie in the range of

$$s^* \in [s^*_{min}, s^*_{max}] \tag{18}$$

$$\equiv \frac{T_{3,in} - T_g}{q_2^* \Delta r} \left[ \frac{1}{i_{AP} + i_{WA}}, \frac{1}{i_{AP}} \right], \tag{19}$$

$$= [0.33, 0.5]^\circ \mathrm{C} \left( \mathrm{Wm}^{-2} \right)^{-1}, \tag{20}$$

which is shaded in the parameter space spanned by global and local sensitivities in Figure 5.

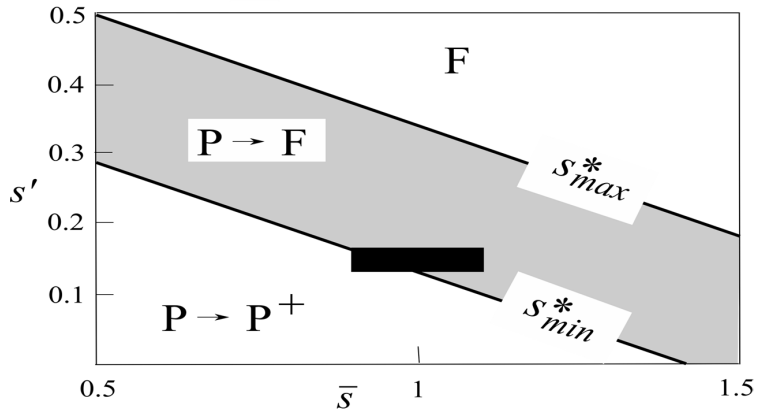


**Figure 5.** Range of the effective sensitivity $s^*$ (shaded) for the observed two-step icing ($P \to F$) on the parameter space of global ($\bar{s}$) and local ($s'$) sensitivities. Above this range, the first icing would fully glaciate Antarctica ($F$) to preclude a second icing, and below this range, the second icing only glaciates West Antarctica ($P \to P^+$). The solid rectangle represents the standard value of sensitivities ($\pm$10%).

Above this range (supercritical), the cooling after the first icing is sufficient to fully glaciate Antarctica ($F$), thus precluding a second icing. Below this range (subcritical), the cooling after the second icing is only sufficient to glaciate West Antarctica ($P \rightarrow P^+$), a minor expansion beyond the Antarctic plateau. Only within the shaded range would there be two-step glaciation from the Antarctic plateau to the entire Antarctica ($P \rightarrow F$), as observed.

The solid rectangle represents the standard sensitivities (with ±10% range) used in calculating the modeled climate shown in Figure 4. Since it lies far below $s^*_{max}$, there is always two-step icing, but since it straddles $s^*_{min}$, whether the second icing leads to full glaciation is more happenstantial. There are indications that climate models might be under-sensitive [10,12], in which case the solid rectangle would move further into the shaded band to augment the likelihood of the observed two-step icing.

## 4. Discussion

I have posited the tectonic origins of the observed two-step Antarctic icing, and to test these hypotheses in the most transparent manner, I have formulated a minimal box model, which is nonetheless physically closed to be prognostic. The neglect of lesser terms does not alter the physical closure to materially impact the model results. On the other hand, the filtering of peripheral parameters lessens the latitude for tuning, and the isolation of key parameters enables a more critical assessment of the model sensitivity, as summarized in Figure 5. Based on this assessment, it is suggested that the two-step icing is robust, but whether the second icing would lead to full glaciation is more happenstantial, which is nonetheless plausible given the representative external parameters.

The physical closure of the model invokes MEP, a generalized second law, which allows the model to be prognostic, representing arguably an advantage over coarse-grained climate models. It should be stressed, however, that MEP does not constitute extraneous physics but merely acknowledges random eddies as a significant carrier of ocean heat [37]. As such, MEP would be entailed in GCMs if they have resolved eddies [38]—a daunting challenge that is often bypassed by tuning subgrid parameterization, such as eddy diffusivity, to the present climate [9,39]. There is, however, no reason why the tuned value should apply to a vastly different paleoclimate, and an alternative more justified approach would be to tune free parameters to maximize the entropy production, thus preserving its prognostic utility [27,40]. Sans MEP, climate models, despite their outward sophistication, may not be used to adjudicate our deductions from a fundamentally different physical closure.

The stability of the Antarctic ice sheet has been widely discussed in the literature in view of the projected anthropogenic warming; my model, however, suggests its considerable stability because of the hysteresis that can be gleaned from Figure 2. That is, cooling would glaciate the Antarctic plateau when SL falls below the plateau (or SST cools to 9 °C) and fully glaciate Antarctica when GL drops to sea level (or SST cools to GMT of 5 °C). Warming-induced deglaciation, however, is subjected to different markers: while ice retreats from the shoreline when SST warms to 5 °C, deglaciation of the Antarctic plateau requires GL (not merely SL) to reach the plateau, or SST warms to 9 °C + 5 °C = 14 °C. This crude estimate is incidentally consistent with that calculated from climate models [14], which suggests extreme warmth is needed for a full deglaciation of Antarctica.

Given the narrow slope flanking the Antarctic plateau, the ice cover assumes only discrete values outside short glacial transitions. This effectively shuts off albedo-temperature feedback in the intervening time to weaken orbital-induced glacial cycles. This feedback was activated during the Pliocene when the ice sheet began to encroach upon contiguous northern lands to amplify obliquity cycles and cause their transition to 100-ky cycles paced by eccentricity [4,27,29]. These glacial cycles naturally have a global reach to imprint on the Antarctic climate, as reflected in periodical collapses of the West Antarctic ice sheet [41].

## 5. Conclusions

The Cenozoic glaciation of Antarctica underwent two distinct steps corresponding to icing of the Antarctic plateau and Antarctica, respectively. I attribute the first icing to the

thermal isolation caused by the opening of the Drake/Tasman passages and the second icing to the uplift of West Antarctica as an isostatic rebound to heightened erosion. To test these hypotheses, I formulated a minimal warm/cold/Antarctic box model to prognose the Antarctic temperature and the associated glacial regimes.

I first distinguished the snowline (SL) delimiting net accumulation and the glacial line (GL) when the net accumulation is depleted by ablation. Depending on the GL relative to sea level, I discerned three equilibrium glacial states of icing over the Antarctic plateau ("partial"), its expansion to West Antarctica ("partial-plus"), and its expansion to the whole Antarctica ("full"). Applying standard parameter values, the modeled time evolution of the Antarctic temperature and associated glacial regime has reproduced the observed two-step icings followed by stabilized temperature levels. I furthermore showed that two-step icing is robust despite uncertain sensitivity, but whether the second icing leads to full glaciation is more happenstantial. With the favorable observational comparison, I suggest that the model has captured the governing physics of the Miocene climate.

**Funding:** This research received no external funding.

**Institutional Review Board Statement:** Not applicable.

**Informed Consent Statement:** Not applicable.

**Data Availability Statement:** No new data were created or analyzed in this study. Data sharing is not applicable since the article describes entirely theoretical research.

**Acknowledgments:** I want to thank the anonymous reviewers for their comments that have improved the paper.

**Conflicts of Interest:** The author declares no conflicts of interest.

## Appendix A. Symbols

| | |
|---|---|
| $a_i$ | Planetary albedo of box-*i* |
| $b$ | Atmospheric absorption (=0.2) |
| $i$ | Ice cover (fraction of cold-box area) |
| $i_{AP}$ | Area of Antarctic plateau (=0.04) |
| $i_{WA}$ | Area of West Antarctica (=0.02) |
| $i_A$ | Area of Antarctica (=0.1) |
| $q_i^*$ | Incoming SW flux of box-*i* |
| $q_i$ | Absorbed SW flux of box-*i* |
| $\overline{q}$ | Global absorbed SW flux |
| $q_c$ | Convective flux |
| $\Delta r$ | Excess reflectance of ice over land |
| $\overline{s}$ | Global sensitivity [=1 $^\circ$C$\left(\mathrm{Wm}^{-2}\right)^{-1}$] |
| $s'$ | Local sensitivity [=0.15 $^\circ$C$\left(\mathrm{Wm}^{-2}\right)^{-1}$] |
| $s^*$ | Effective sensitivity [$\equiv(\overline{s}+3s')/4=0.36$ $^\circ$C$\left(\mathrm{Wm}^{-2}\right)^{-1}$] |
| $s^*_{max}$ | Maximum $s^*$ for partial-to-full icing [=0.5 $^\circ$C$\left(\mathrm{Wm}^{-2}\right)^{-1}$] |
| $s^*_{min}$ | Minimum $s^*$ for partial-to-full icing [=0.33 $^\circ$C$\left(\mathrm{Wm}^{-2}\right)^{-1}$] |
| $T_g$ | Glacial marking temperature (=5 $^\circ$C) |
| $T_i$ | SST (same as summer SAT) of box-*i* |
| $T_{3,in}$ | Initial Antarctic SST at EOB (=9 $^\circ$C) |

| | |
|---|---|
| $T_{a,i}$ | SAT of box-$i$ |
| $y$ | Latitudinal distance $\equiv \sin(\text{latitude})$ |
| $\alpha$ | Air-sea exchange coefficient $(=10\ \text{Wm}^{-2\circ}\text{C}^{-1})$ |
| $\gamma$ | Lapse rate $(=6\ ^\circ\text{C km}^{-1})$ |
| $\sigma_a$ | Atmospheric entropy production |
| $\sigma_o$ | Oceanic entropy production |

## References


1. Cramer, B.S.; Miller, K.G.; Barrett, P.J.; Wright, J.D. Late Cretaceous–Neogene trends in deep ocean temperature and continental ice volume: Reconciling records of benthic foraminiferal geochemistry (δ18O and Mg/Ca) with sea level history. *J. Geophys. Res. Oceans* **2011**, *116*, C12023. [CrossRef]
2. Kennett, J.P. Cenozoic evolution of Antarctic glaciation, the circum-Antarctic oceans and their impact on global paleoceanography. *J. Geophys. Res.* **1977**, *82*, 3843–3859. [CrossRef]
3. Toggweiler, J.R.; Bjornsson, H. Drake Passage and palaeoclimate. *J. Quat. Sci.* **2000**, *15*, 319–328. [CrossRef]
4. Zachos, J.; Pagani, M.; Sloan, L.; Thomas, E.; Billups, K. Trends, rhythms, and aberrations in global climate 65 Ma to present. *Science* **2001**, *292*, 686–693. [CrossRef]
5. Ou, H.W. Northern Hemisphere Glaciation: Its Tectonic Origin in the Neogene Uplift. *Glacies* **2024**, *1*, 19–34. [CrossRef]
6. Ohmura, A. New temperature distribution maps for Greenland. *Z. Für. Gletscherkunde Und Glazialgeol.* **1987**, *23*, 1–45.
7. Miller, K.G.; Fairbanks, R.G.; Mountain, G.S. Tertiary oxygen isotope synthesis, sea level history, and continental margin erosion. *Paleoceanography* **1987**, *2*, 1–19. [CrossRef]
8. Scher, H.D.; Martin, E.E. Timing and climatic consequences of the opening of Drake Passage. *Science* **2006**, *312*, 428–430. [CrossRef] [PubMed]
9. De Conto, R.D.; Pollard, D. Rapid Cenozoic glaciation of Antarctica triggered by declining atmospheric $CO_2$. *Nature* **2003**, *421*, 245–249. [CrossRef]
10. Gasson, E.G.W.; Keisling, B.A. The Antarctic Ice Sheet: A paleoclimate modeling perspective. *Oceanography* **2020**, *33*, 90–100. [CrossRef]
11. Halberstadt, A.R.; Chorley, H.; Levy, R.H.; Naish, T.; DeConto, R.M.; Gasson, E.; Kowalewski, D.E. $CO_2$ and tectonic controls on Antarctic climate and ice-sheet evolution in the mid-Miocene. *Earth Planet Sci. Lett.* **2021**, *564*, 116908. [CrossRef]
12. McKay, R.M.; Escutia, C.; De Santis, L.; Donda, F.; Duncan, B.; Gohl, K.; Gulick, S.; Hernández-Molina, J.; Hillenbrand, C.D.; Hochmuth, K.; et al. Cenozoic history of Antarctic glaciation and climate from onshore and offshore studies. In *Antarctic Climate Evolution*; Elsevier: Amsterdam, The Netherlands, 2022; pp. 41–164. [CrossRef]
13. Meehl, G.A.; Senior, C.A.; Eyring, V.; Flato, G.; Lamarque, J.F.; Stouffer, R.J.; Taylor, K.E.; Schlund, M. Context for interpreting equilibrium climate sensitivity and transient climate response from the CMIP6 Earth system models. *Sci. Adv.* **2020**, *6*, eaba1981. [CrossRef] [PubMed]
14. Huybrechts, P. Glaciological modelling of the Late Cenozoic East Antarctic ice sheet: Stability or dynamism? *Geogr. Ann. Ser. A Phys. Geogr.* **1993**, *75*, 221–238. [CrossRef]
15. Lemasurier, W.E.; Rocchi, S. Terrestrial record of post-eocene climate history in marie byrd land, west antarctica. *Geogr. Ann. Ser. A Phys. Geogr.* **2005**, *87*, 51–66. [CrossRef]
16. Rocchi, S.; LeMasurier, W.; Di Vicenzo, G. Oligocene to Holocene erosion and glacial history in Marie Byrd Land, West Antarctica, inferred from exhumation of the Dorrel rock intrusive complex and from volcano morphologies. *Geol. Soc. Am. Bull.* **2006**, *118*, 991–1005. [CrossRef]
17. Spiegel, C.; Lindow, J.; Kamp, P.J.; Meisel, O.; Mukasa, S.; Lisker, F.; Kuhn, G.; Gohl, K. Tectonomorphic evolution of Marie Byrd Land–Implications for Cenozoic rifting activity and onset of West Antarctic glaciation. *Glob. Planet. Change* **2016**, *145*, 98–115. [CrossRef]
18. Paxman, G.J.G.; Jamieson, S.S.R.; Hochmuth, K.; Gohl, K.; Bentley, M.J.; Leitchenkov, G.; Ferraccioli, F. Reconstructions of Antarctic topography since the Eocene–Oligocene boundary. *Palaeogeogr. Palaeoclimatol. Palaeoecol.* **2019**, *535*, 109346. [CrossRef]
19. Behrendt, J.C.; Cooper, A. Evidence of rapid Cenozoic uplift of the shoulder escarpment of the Cenozoic West Antarctic rift system and a speculation on possible climate forcing. *Geology* **1991**, *19*, 315–319. [CrossRef]
20. Fitzgerald, P. Tectonics and landscape evolution of the Antarctic plate since the breakup of Gondwana, with an emphasis on the West Antarctic Rift system and the Transantarctic Mountains. *R. Soc. N. Z. Bull.* **2002**, *35*, 453–469.
21. Peixoto, J.P.; Oort, A.H. *Physics of Climate*; American Institute of Physics: New York, NY, USA, 1992; 520p.
22. Ou, H.W. Meridional thermal field of a coupled ocean-atmosphere system: A conceptual model. *Tellus A* **2006**, *58*, 404–415. [CrossRef]
23. Ou, H.W. Thermohaline circulation: A missing equation and its climate change implications. *Clim. Dyn.* **2018**, *50*, 641–653. [CrossRef]

24. Ozawa, H.; Ohmura, A.; Lorenz, R.D.; Pujol, T. The second law of thermodynamics and the global climate system: A review of the maximum entropy production principle. *Rev. Geophys.* **2003**, *41*, 10182003. [CrossRef]
25. Kleidon, A. Non-equilibrium thermodynamics and maximum entropy production in the Earth system: Applications and implications. *Naturwissenschaften* **2009**, *96*, 653–677. [CrossRef] [PubMed]
26. Kucera, M.; Weinelt, M.; Kiefer, T.; Pflaumann, U.; Hayes, A.; Weinelt, M.; Chen, M.T.; Mix, A.C.; Barrows, T.T.; Cortijo, E.; et al. Reconstruction of sea-surface temperatures from assemblages of planktonic foraminifera: Multi-technique approach based on geographically constrained calibration data sets and its application to glacial Atlantic and Pacific Oceans. *Quat. Sci. Rev.* **2005**, *24*, 951–998. [CrossRef]
27. Ou, H.W. A theory of orbital-forced glacial cycles: Resolving Pleistocene puzzles. *J. Mar. Sci. Eng.* **2023**, *11*, 564. [CrossRef]
28. Macdonald, A.M. The global ocean circulation: A hydrographic estimate and regional analysis. *Prog. Oceanogr.* **1998**, *41*, 281–382. [CrossRef]
29. Hansen, J.; Sato, M.; Russell, G.; Kharecha, P. Climate sensitivity, sea level and atmospheric carbon dioxide. *Phil. Trans. R. Soc. A* **2013**, *371*, 20120294. [CrossRef]
30. Goldner, A.; Huber, M.; Caballero, R. Does Antarctic glaciation cool the world? *Clim. Past.* **2013**, *9*, 173–189. [CrossRef]
31. Haq, B.U.; Hardenbol, J.A.; Vail, P.R. Chronology of fluctuating sea levels since the Triassic. *Science* **1987**, *235*, 1156–1167. [CrossRef]
32. Flower, B.P.; Kennett, J.P. The middle Miocene climatic transition: East Antarctic ice sheet development, deep ocean circulation and global carbon cycling. *Palaeogeogr. Palaeoclimatol. Palaeoecol.* **1994**, *108*, 537–555. [CrossRef]
33. Wilson, D.S.; Pollard, D.; DeConto, R.M.; Jamieson, S.S.R.; Luyendyk, B.P. Initiation of the West Antarctic Ice Sheet and estimates of total Antarctic ice volume in the earliest Oligocene. *Geophys. Res. Lett.* **2013**, *40*, 4305–4309. [CrossRef]
34. Bart, P.J. Were West Antarctic ice sheet grounding events in the Ross Sea a consequence of East Antarctic ice sheet expansion during the middle Miocene? *Earth Planet. Sci. Lett.* **2003**, *216*, 93–107. [CrossRef]
35. Pierce, E.L.; van de Flierdt, T.; Williams, T.; Hemming, S.R.; Cook, C.P.; Passchier, S. Evidence for a dynamic East Antarctic ice sheet during the mid-Miocene climate transition. *Earth Planet. Sci. Lett.* **2017**, *478*, 1–13. [CrossRef]
36. Barrett, P. Resolving views on Antarctic Neogene glacial history—The Sirius debate. *Earth Environ. Sci. Trans. R. Soc. Edinburgh* **2013**, *104*, 31–53. [CrossRef]
37. Lozier, M.S. Deconstructing the conveyer belt. *Science* **2010**, *328*, 1507–1511. [CrossRef]
38. Liu, T.; Ou, H.W.; Liu, X.; Chen, D. On the role of eddy mixing in the subtropical ocean circulation. *Front. Mar. Sci.* **2022**, *9*, 832992. [CrossRef]
39. Rahmstorf, S.; Crucifix, M.; Ganopolski, A.; Goosse, M.; Kamenkovich, I.; Knutti, R.; Lohmann, G.; Marsh, R.; Mysak, L.A.; Wang, Z.; et al. Thermohaline circulation hysteresis: A model intercomparison. *Geophys. Res. Lett.* **2005**, *32*, L23605. [CrossRef]
40. Kunz, T.; Fraedrich, K.; Kirk, E. Optimisation of simplified GCMs using circulation indices and maximum entropy production. *Clim. Dyn.* **2008**, *30*, 803–813. [CrossRef]
41. Naish, T.; Powell, R.; Levy, R.; Wilson, G.; Scherer, R.; Talarico, F.; Krissek, L.; Niessen, F.; Pompilio, M.; Wilson, T.; et al. Obliquity-paced Pliocene West Antarctic ice sheet oscillations. *Nature* **2009**, *458*, 322–328. [CrossRef]